ChemPubSoc Europe

DOI: 10.1002/chem.201601648

CHEMISTRY A European Journal Full Paper

Oxidation Reactions

Acceptorless Dehydrogenative Oxidation of Secondary Alcohols Catalysed by Cp*Ir^{III}–NHC Complexes**

Süleyman Gülcemal,[a, b] Derya Gülcemal,*[a, b] George F. S. Whitehead,[a] and Jianliang Xiao*[a]

Abstract: A series of new Ir^{III} complexes with carbene ligands that contain a range of benzyl wingtip groups have been prepared and fully characterised by NMR spectroscopy, HRMS, elemental analysis and X-ray diffraction. All the complexes were active in the acceptorless dehydrogenation of alcohol substrates in 2,2,2-trifluoroethanol to give the corresponding carbonyl compounds. The most active complex bore an electron-rich carbene ligand; this complex was used to catalyse the highly efficient and chemoselective dehydrogenation of a wide range of secondary alcohols to their respective ketones, with turnover numbers up to 1660. Mechanistic studies suggested that the turnover of the dehydrogenation reaction is limited by the H_2-formation step.

Introduction

N-Heterocyclic carbenes (NHCs) have emerged as a versatile class of ligands in organometallic chemistry and catalysis. NHCs often form stable complexes with transition metals irrespective of their oxidation states[1] Additionally, their tunable character allows for easy control of the electronic and steric properties at the metal centre. Recently, transition-metal/NHC complexes have found applications in acceptorless dehydrogenative β-alkylation,[2] amidation,[3] *N*-formylation[4] and imine formation reactions.[5] However, there are only a few reported examples of NHC-based complexes that catalyse the acceptorless dehydrogenative oxidation of alcohols to afford carbonyl compounds.[6] In these reports, the acceptorless dehydrogenation (AD) reactions are typically carried out at reflux temperature in high-boiling solvents, such as toluene, and full conversion of the alcohol to the corresponding carbonyl compound requires high catalytic loadings (2–5 mol%) and furnishes maximum turnover numbers (TONs) of only 50.

Oxidation of alcohols to carbonyl compounds is one of the most fundamental reactions in organic synthesis, both in academic laboratories and industrial processes to access chemicals, fuels and pharmaceuticals. The removal of hydrogen from a hydrogen-rich organic molecule is often a thermodynamically unfavourable process. Thus, conventional dehydrogenation reactions are typically carried out by using stoichiometric- or excess amounts of metal-based oxidants. Environmentally acceptable oxidants such as molecular oxygen,[7] hydrogen peroxide[8] and, less desirably, acetone[9] have been used in catalytic oxidation reactions. However, from an atom-efficiency and environmental viewpoint, the oxidant-free AD reaction is more desirable because H_2 is released as a gas.[10]

Herein, we report the synthesis and characterisation of a range of Cp*Ir^{III}–NHC complexes (Cp* = 1,2,3,4,5-pentamethylcyclopentadienyl) with different benzyl substituents and azole skeletons. These complexes are active catalysts for the AD of secondary benzylic and aliphatic alcohols to ketones in 2,2,2-trifluoroethanol (TFE; b.p. 78 °C) at reflux temperature, with TONs up to 1660. To the best of our knowledge, this is one of the highest TONs obtained for the AD of secondary alcohols to the corresponding ketones promoted by an NHC-containing catalyst, as well as the first example of Cp*Ir^{III}–NHC catalysts for these transformations. It is noted, however, that transition-metal complexes bearing C–N, NCN and PCP pincer ligands have been reported to be efficient catalysts for the AD of primary and secondary alcohols.[11–15]

Results and Discussion

Scheme 1 outlines the route used for the synthesis of [Cp*Ir(NHC)Cl$_2$] complexes **2a**–**f**. The new Cp*Ir^{III}–NHC complexes **2a**–**f** were prepared in high yields as air- and moisture-stable yellow solids by a two-step process that involved transmetallation[16] from the Ag–NHC derivatives formed in situ, (Scheme 1). Complexes **2a**–**f** were characterised by NMR spectroscopy, HRMS and elemental analysis. Complexes **2a**–**f** exhibit ^{13}C NMR chemical shifts at δ = 156.5, 157.5, 158.7, 186.5, 172.0 and 161.9 ppm, respectively, for the characteristic Ir–$C_{carbene}$ carbon atom, and the values are comparable to those of other reported Cp*Ir^{III}–NHC complexes with an azole skeleton.[9c–e, 17] Meanwhile, the characteristic downfield signals for

[a] Prof. S. Gülcemal, Prof. D. Gülcemal, Dr. G. F. S. Whitehead, Prof. J. Xiao
Department of Chemistry, University of Liverpool
Liverpool, L69 7ZD (UK)
E-mail: jxiao@liv.ac.uk

[b] Prof. S. Gülcemal, Prof. D. Gülcemal
Department of Chemistry, Ege University
35100 Bornova-Izmir (Turkey)
E-mail: suleyman.gulcemal@ege.edu.tr

[**] Cp* = 1,2,3,4,5-pentamethylcyclopentadienyl, NHC = N-heterocyclic carbene.

Supporting information for this article is available on the WWW under http://dx.doi.org/10.1002/chem.201601648.

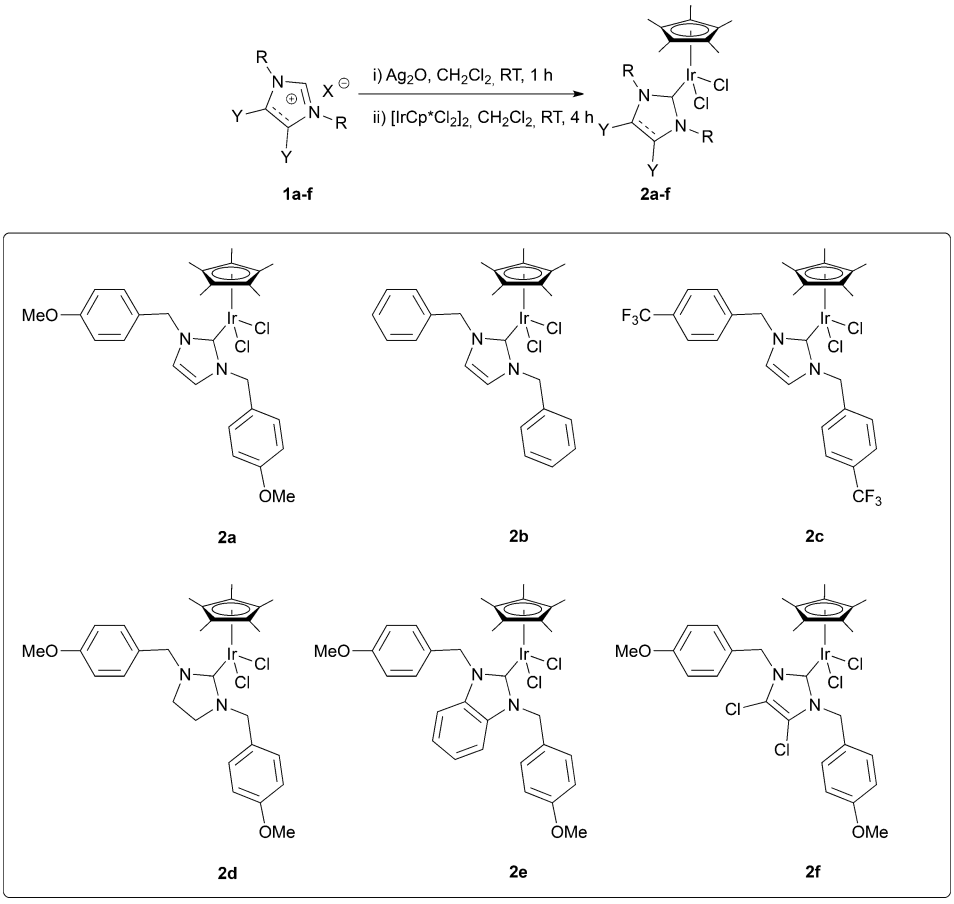

Scheme 1. Synthesis of the Cp*Ir^{III}–NHC complexes **2a–f** used in this study.

the NCHN$^+$ proton of azolium salts **1a–f** disappeared in the ^{1}H NMR spectrum. Finally, the molecular structure of all the complexes was determined by single-crystal X-ray diffraction. Single crystals were obtained by diffusion of pentane into concentrated solutions of the complexes in chloroform. Coordination of a single NHC to the iridium centre was confirmed (Figures 1–6; atom-numbering and selected bond lengths [Å] and angles [°] are shown). All the complexes exhibit piano-stool type geometry. The Ir–$C_{carbene}$ bond lengths (2.065(5)–2.023(6) Å) are in the expected range,[9c–e,17] and are slightly longer with more electron-rich NHC ligands.

We started the investigation with 1-phenylethanol (**3a**) as a model substrate and TFE as the solvent for the AD reaction catalysed by **2a**. TFE has been shown to be a most effective solvent for the AD of heterocycles catalysed by cyclometallated Cp*Ir^{III}, possibly by promoting the dissociation of chloride from the complex and, hence, promoting coordination of the substrate to the metal centre and protonation of the intermediate hydride to facilitate H_2 formation.[18] The AD of **3a** under various conditions was examined first (Table 1). When a solution of **3a** in TFE was heated at reflux for 2 h in the presence of **2a** (1.0 mol%), we observed the formation of acetophenone (**4a**) and also, unexpectedly, fluorinated ether (**5**) (**3a**/**4a**/**5** = 66:20:14; Table 1, entry 1). Addition of $NaBF_4$ or NH_4BF_4 (5.0 mol%) increased the amount of undesired product **5**

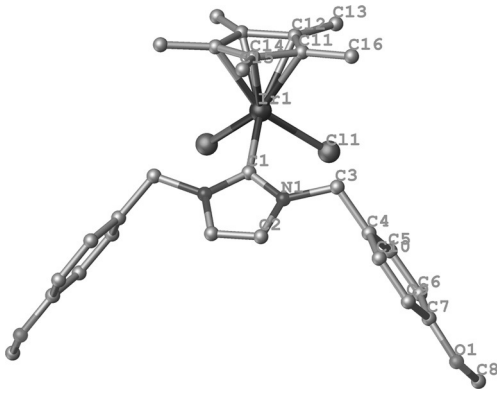

Figure 1. Molecular structure of **2a** with hydrogen atoms removed for clarity. Selected bond lengths [Å] and angles [°]: Ir(1)–C(1) 2.059(5), Ir(1)–Cl(1) 2.4399(10), C(1)–N(1) 1.374(4), C(2)–N(1) 1.392(4); C(1)-Ir(1)-Cl(1) 91.38(11), C(1)-N(1)-C(2) 111.2(3).

(Table 1, entries 2 and 3). This could result from the formation of acidic HF, which would be expected to catalyse the etherisation of **3a** by TFE.[19] Hence, the reaction was examined by introducing different bases (5.0 mol%) to suppress etherisation (Table 1, entries 4–8). Indeed, **5** was not detected when a base was introduced, and pleasingly, in the presence of NaOAc, the

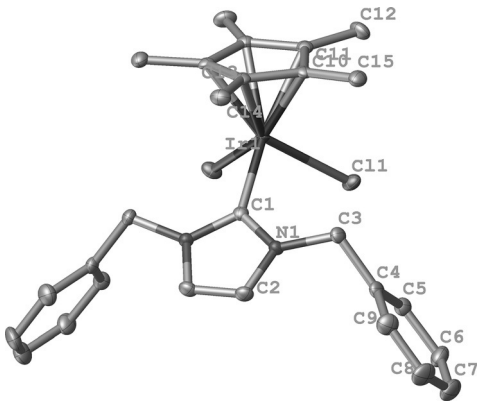

Figure 2. Molecular structure of **2b** with hydrogen atoms removed for clarity. Selected bond lengths [Å] and angles [°]: Ir(1)–C(1) 2.055(6), Ir(1)–Cl(1) 2.4300(9), C(1)–N(1) 1.367(6), C(2)–N(1) 1.395(6); C(1)-Ir(1)-Cl(1) 92.09(11), C(1)-N(1)-C(2) 111.6(4).

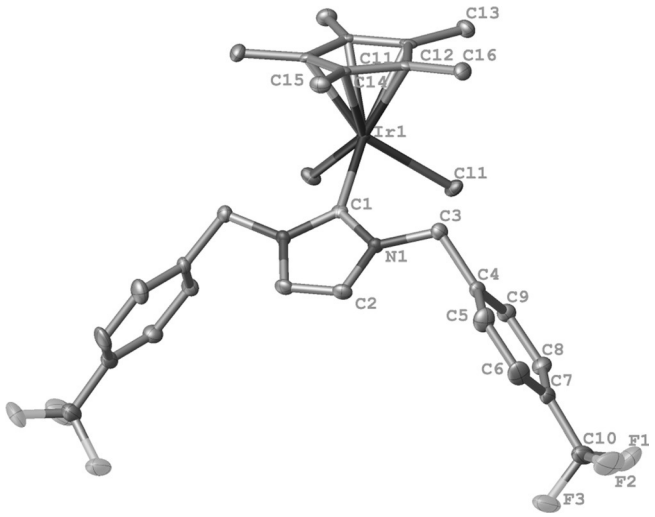

Figure 3. Molecular structure of **2c** with hydrogen atoms removed for clarity. Selected bond lengths [Å] and angles [°]: Ir(1)–C(1) 2.051(4), Ir(1)–Cl(1) 2.4383(7), C(1)–N(1) 1.364(3), C(2)–N(1) 1.385(3); C(1)-Ir(1)-Cl(1) 91.36(8), C(1)-N(1)-C(2) 111.5(2).

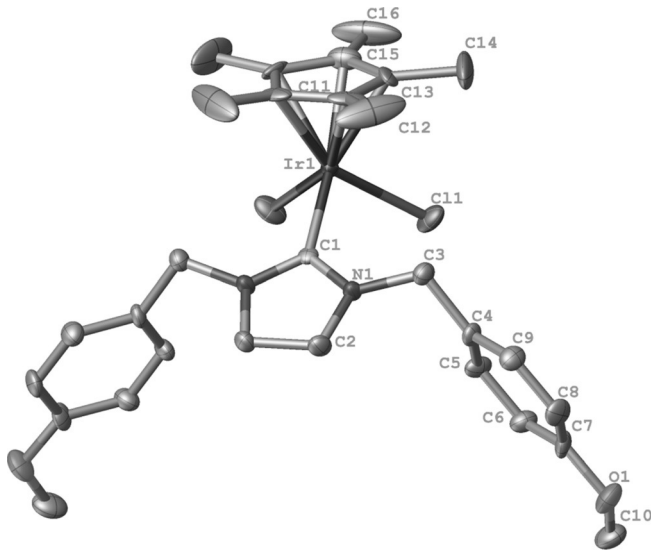

Figure 4. Molecular structure of **2d** with hydrogen atoms removed for clarity. Selected bond lengths [Å] and angles [°]: Ir(1)–C(1) 2.065(6), Ir(1)–Cl(1) 2.4182(12), C(1)–N(1) 1.345(5), C(2)–N(1) 1.468(6); C(1)-Ir(1)-Cl(1) 92.93(12), C(1)-N(1)-C(2) 113.6(4).

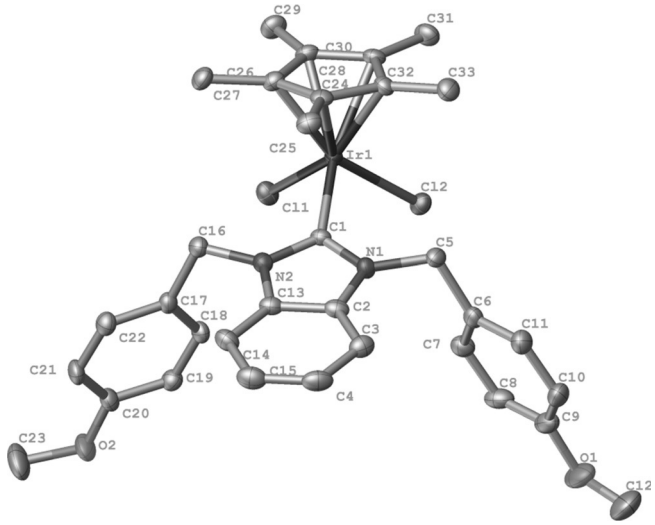

Figure 5. Molecular structure of **2e** with hydrogen atoms and chloroform solvent removed for clarity. Selected bond lengths [Å] and angles [°]: Ir(1)–C(1) 2.029(3), Ir(1)–Cl(2) 2.4054(9), C(1)–N(1) 1.373(4), C(2)–N(1) 1.397(5); C(1)-Ir(1)-Cl(2) 93.23(10), C(1)-N(1)-C(2) 110.8(3).

conversion to **4a** increased to 82% (Table 1, entry 6>). Complete conversion to **4a** was achieved in the presence of **2a** (0.1 mol%) and NaOAc (5.0 mol%) after 20 h (Table 1, entry 9). However, further decreasing the catalyst loading (0.05 mol%) resulted in a lower conversion (77%) after 20 h (Table 1, entry 10). The amount of NaOAc was also found to affect the rate of the AD reaction (Table 1, entries 11–13): the highest conversion to **4a** was obtained in the presence of NaOAc (2.5 mol%) (83%, TON = 1660; Table 1, entry 12). By using this lower amount of base, full conversion was obtained with a lower catalyst loading (0.1 mol%; Table 1, entry 14).

Other iridium complexes with different NHC ligands (**2b**–**e**) were subsequently evaluated under the same reaction conditions. Complex **2a**, which bore a 1,3-bis(4-methoxybenzyl)-imidazol-2-ylidene ligand, provided the highest conversion (Table 1, entries 14–19). It is clear that both the electronic effect of the wingtip (*p*-OMe, *p*-H and *p*-CF_3) and the type of NHC skeleton are important for the AD reaction. Comparison of the conversions obtained with sterically similar complexes **2a**–**c** indicates that the more electron rich the iridium centre is, the higher the catalytic activity. In contrast, only 3% conversion was obtained with $[IrCl_2Cp^*]_2$ under the same conditions, which shows the importance of the NHC ligand for the AD reaction (Table 1, entry 20). A control experiment was carried out without any catalyst and no product formation was observed (Table 1, entry 21). Notably, when the AD reaction was carried out in a closed system only 62% yield of **4a** was achieved (Table 1, entry 22), which indicates that the AD reaction is re-

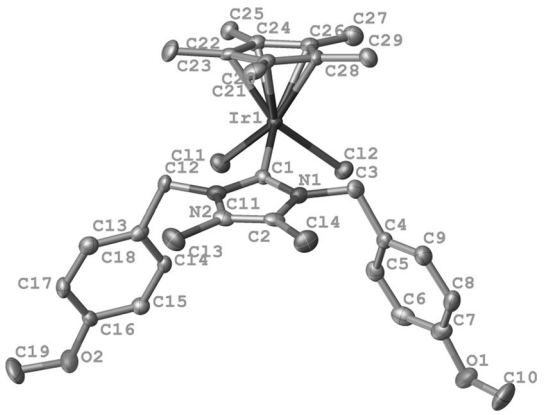

Figure 6. Molecular structure of **2 f** with hydrogen atoms and chloroform solvent removed for clarity. Selected bond lengths [Å] and angles [°]: Ir(1)–C(1) 2.023(6), Ir(1)–Cl(2) 2.3909(16), C(1)–N(1) 1.378(7), C(2)–N(1) 1.381(8); C(1)-Ir(1)-Cl(2) 93.21(17), C(1)-N(1)-C(2) 110.5(5).

Table 1. Cp*Ir^{III}–NHC catalysed AD of **3 a** in TFE.[a]

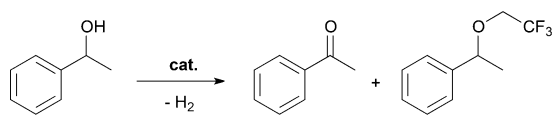

3a **4a** **5**

Entry	Cat. [mol% Ir]	Solvent	Additive [mol %]	Time [h]	**3 a**/**4 a**/**5** [%][b]
1	**2 a** (1.0)	TFE	–	2	66:**20**:14
2	**2 a** (1.0)	TFE	$NaBF_4$ (5.0)	2	10:**10**:80
3	**2 a** (1.0)	TFE	NH_4BF_4 (5.0)	2	0:**13**:87
4	**2 a** (1.0)	TFE	$NaHCO_3$ (5.0)	2	59:**41**:0
5	**2 a** (1.0)	TFE	Na_2CO_3 (5.0)	2	56:**44**:0
6	**2 a** (1.0)	TFE	NaOAc (5.0)	2	18:**82**:0
7	**2 a** (1.0)	TFE	KOAc (5.0)	2	31:**69**:0
8	**2 a** (1.0)	TFE	AgOAc (5.0)	2	40:**60**:0
9	**2 a** (0.1)	TFE	NaOAc (5.0)	20	0:**100**:0
10	**2 a** (0.05)	TFE	NaOAc (5.0)	20	23:**77**:0
11	**2 a** (0.05)	TFE	NaOAc (10)	20	55:**45**:0
12	**2 a** (0.05)	TFE	NaOAc (2.5)	20	17:**83**:0
13	**2 a** (0.05)	TFE	NaOAc (1.0)	20	29:**71**:0
14	**2 a** (0.1)	TFE	NaOAc (2.5)	20	0:**100**:0
15	**2 b** (0.1)	TFE	NaOAc (2.5)	20	21:**79**:0
16	**2 c** (0.1)	TFE	NaOAc (2.5)	20	69:**31**:0
17	**2 d** (0.1)	TFE	NaOAc (2.5)	20	7:**93**:0
18	**2 e** (0.1)	TFE	NaOAc (2.5)	20	85:**15**:0
19	**2 f** (0.1)	TFE	NaOAc (2.5)	20	54:**46**:0
20	$[IrCl_2Cp^*]_2$ (0.1)	TFE	NaOAc (2.5)	20	97:**3**:0
21	–	TFE	NaOAc (2.5)	20	100:0:0
22[c]	**2 a** (0.1)	TFE	NaOAc (2.5)	20	38:**62**:0
23[d]	**2 a** (0.1)	TFE	NaOAc (2.5)	20	13:**87**:0
24	**2 a** (0.1)	toluene	NaOAc (2.5)	20	98:**2**:0
25	**2 a** (0.1)	EtOH	NaOAc (2.5)	20	100:0:0
26	**2 a** (0.1)	HFIP	NaOAc (2.5)	20	11:**89**:0

[a] Reaction conditions: alcohol (1 mmol), **2** (0.05–1.0 mol%), additive (1-10 mol%), TFE (1 mL), N_2, reflux. [b] Conversion determined from the ^{1}H NMR spectrum. [c] Reaction performed in a closed system. [d] Reaction vessel was open to air.

versible and is facilitated by the release of H_2. In addition, we detected the evolution of H_2 gas during the dehydrogenation of **3 a** by GC analysis.[20] However, performing the AD reaction under an ambient atmosphere also resulted in a lower conversion (87%; Table 1, entry 23). This could be due to the intermediate iridium–hydride species being unstable toward O_2.[21] The use of TFE is critical for the reaction to proceed; very little or no reaction was observed with the other solvents tested (Table 1, entries 24 and 25). This is reminiscent of the observations made for iridicycles in the AD of N-heterocycles and suggests that the formation of H_2, which is facilitated by acidic TFE ($pK_a = 12.5$), may be turnover limiting,.[18] Consistent with this, the AD reaction was slightly faster when an alcohol of lower acidity was used as the solvent, for example, hexafluoroisopropanol (HFIP, $pK_a = 9.3$) (Table 1, entry 26).

The ability of Cp*Ir^{III}–NHC complexes to undergo intramolecular aromatic C–H activation was reported by Peris and coworkers.[22] They reported that, in most cases, the *ortho*-metallation occurs under very mild conditions. To investigate the possible effect of *ortho*-metallation on the AD reaction, we studied the reaction of complex **2 a** with NaOAc (5 equiv) in dichloromethane (Scheme 2). We found that **2 a** was converted to a new complex **2 a′**, which could be isolated in 90% yield. Comparison of the ^{1}H NMR spectra of **2 a** and **2 a′** suggests that complex **2 a′** could arise from intramolecular aromatic C–H activation. The CH_2 protons of the benzyl groups display signals at $\delta = 6.03$ (d, $J = 14.4$ Hz, 2H) and 5.10 ppm (d, $J = 14.4$ Hz, 2H) for **2 a** and at $\delta = 5.95$ (d, $J = 14.0$ Hz, 1H), 4.99 (d, $J = 14.0$ Hz, 1H), 4.83 (d, $J = 14.0$ Hz, 1H) and 4.62 ppm (d, $J = 14.0$ Hz, 1H) for **2 a′**, which is consistent with the *ortho*-metallation results previously reported.[17b,22] The ^{13}C NMR spectrum of **2 a′** also supports that *ortho*-metallation has occurred: the additional Ir–C_{Ar} signal is observed at $\delta = 146.1$ ppm.[17b,22] Furthermore, crystals of complex **2 a′** suitable for X-ray diffraction were obtained by diffusion of pentane into a concentrated solution of **2 a′** in chloroform, and the proposed structure was confirmed (Figure 7). As can be seen (Figure 7), *ortho*-metallation of the phenyl ring of the imidazol-2-ylidene ligand has occurred, which leads to a chelating coordination of the ligand. The Ir–$C_{carbene}$ and Ir–C_{phenyl} bond lengths are 2.05 and 2.04 Å, respectively, and lie in the expected range.[17b,22]

Complex **2 a′** was evaluated as a catalyst for the AD reaction of **3 a** by using the conditions described in Table 1, entry 14.

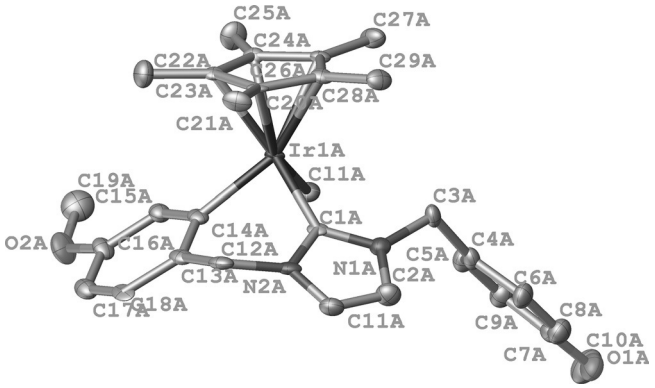

Figure 7. Molecular structure of **2 a′** with hydrogen atoms removed for clarity. Selected bond lengths [Å] and angles [°]: Ir(1A)–C(1A) 2.050(13), Ir(1A)–C(14A) 2.040(13), Ir(1A)–Cl(1A) 2.428(5); C(1A)-Ir(1A)-C(14A) 85.1(5), C(1A)-Ir(1A)-Cl(1A) 92.5(4), C(14A)-Ir(1A)-Cl(1A) 88.0(4).

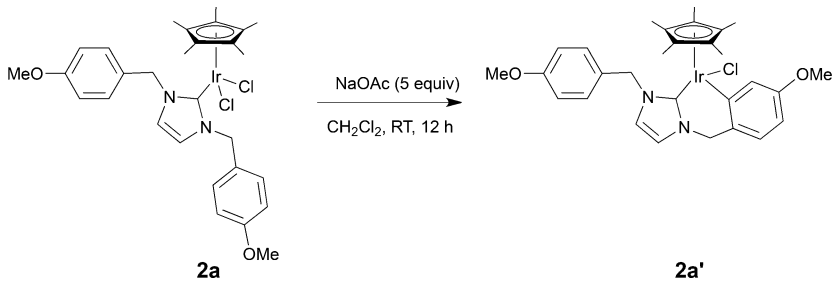

Scheme 2. Synthesis of the *ortho*-metallated Cp*Ir^{III}–NHC complex **2a**′.

Good conversion (80%) to **4a** was achieved in the presence of **2a**′ (0.1 mol%) and NaOAc (2.5 mol%) after 20 h. The results show that catalyst **2a** is more active than the *ortho*-metallated analogue **2a**′ (cf. Table 1, entry 14), which suggests that *ortho*-metallation does not play a significant role, if any, in the AD reaction.

To explore the scope of the present catalytic AD system, the reactions of a wide range of secondary alcohols were conducted under the optimised conditions (Table 2). Various 1-arylethanols (**3a**–**e**) bearing electron-donating or electron-withdrawing substituents at the *para*-position of the phenyl ring were effectively converted into the corresponding ketones (**4a**–**e**) in high yields by using **2a** (0.1 mol%) as the catalyst (Table 2, entries 1–5). Only *para*-CF_3-substituted 1-arylethanol **3e** gave a lower conversion and isolated yield (Table 2, entry 5). More sterically hindered 1-arylalcohols **3f**–**n** gave the corresponding ketones **4f**–**n** in 83–98% isolated yield (Table 2, entries 6–14). In addition to the aromatic substrates, aliphatic secondary alcohols **3o**–**s** were dehydrogenated to give aliphatic ketones **4o**–**s** (Table 2, entries 15–19). However, some of these substrates required a higher catalyst loading, probably due to subtle steric effects (for example, Table 2, entries 6–8, 15, 17 and 18).

Next, we examined the AD of primary alcohols. However, the AD of benzyl alcohol (**6**) (1.0 mmol) in the presence of **2a** (1.0 mol%) did not proceed well: only 18% conversion to benzaldehyde (**7**) was observed by NMR spectroscopy (Scheme 3). Considering that the AD reaction may be reversible and that aldehydes are easier to reduce than ketones, the low conversion to **7** could be a result of the product being reduced under the AD conditions. In fact, AD can be seen as a transfer-hydrogenation reaction, in which the removed hydrogen atom is not captured by a sacrificial acceptor but released from the reaction.[10f] To show the possibility of **2a** catalysing the reverse reaction of primary alcohol dehydrogenation, we examined its activity toward the hydrogenation of **7**. Indeed, we found that **2a** (0.1 mol%) catalysed the quantitative hydrogenation of **7** (1.0 mmol) to **6** under a balloon of H_2 (1 atm) in TFE at 40 °C after 4 h (Scheme 3). Further evidence of the reversibility of the AD of **6** is the AD of **7** during the dehydrogenation of **3a** (Scheme 4). When a mixture of **3a** (1.0 mmol) and **7** (1.0 mmol) was subjected to the AD reaction conditions with **2a** (0.25 mol% relative to **3a**) **3a** was fully converted into **4a**, whereas **7** was reduced to **6** in 96% conversion by "borrowing" the hydrogen atom from **3a** (Scheme 4).[23] These results also show that **2a** is an active catalyst for both hydrogenation and-transfer hydrogenation reactions, and indicate that the low efficiency of **2a** in the AD of **6** is due to easier reduction of the product.

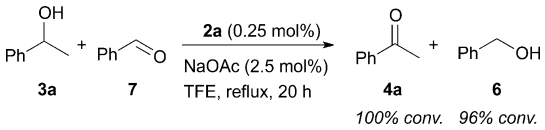

Scheme 4. Intermolecular hydrogen transfer process.

The reversibility of the AD of primary alcohols can be exploited for chemoselective AD reactions. For example, the AD of **3a** (1.0 mmol) and **6** (1.0 mmol) with catalyst **2a** (0.25 mol%) resulted in full conversion of **3a** to **4a**, but only 3% conversion of **6** to **7** after 20 h (Scheme 5), which demonstrates the excellent selectivity of the catalyst for secondary versus primary benzylic alcohols.

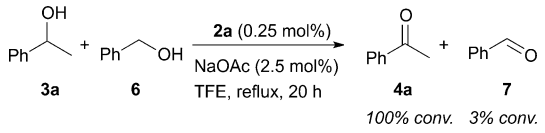

Scheme 5. Selective dehydrogenation of secondary alcohols.

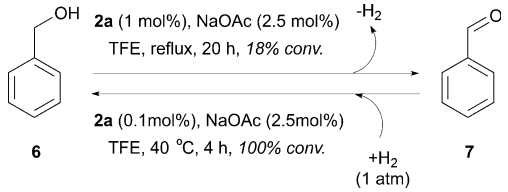

Scheme 3. Reversible AD of primary alcohol **6**.

Furthermore, we investigated the AD of diols, which can potentially release two equivalents of H_2 to form stable lactones.[11c,12b,15c,24] Thus, in the presence of **2a** (1.0 mol%) and NaOAc (5.0 mol%), 1,2-dibenzenedimethanol (**8a**) and 1,5-pentanediol (**8b**) were converted into the corresponding lactones—phthalide (**9a**) and δ-valerolactone (**9b**)—in 95 and

Table 2. AD of various secondary alcohols catalysed by **2a**.[a]

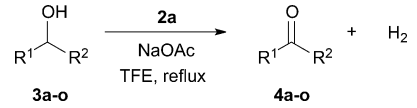

Entry	Product		S/C[b]	Conv. [%][c]	Yield [%][d]
1		**4a**	1000	100	96
2	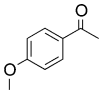	**4b**	1000	100	97
3		**4c**	1000	100	94
4	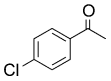	**4d**	1000	98	91
5	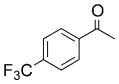	**4e**	1000	84	81
6		**4f**	500	96	93
7		**4g**	500	93	88
8		**4h**	500	100	97
9	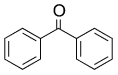	**4i**	1000	100	98
10	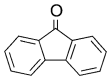	**4j**	1000	86	83
11	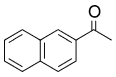	**4k**	1000	100	97
12		**4l**	1000	100	95
13		**4m**	1000	100	97
14		**4n**	1000	92	87
15		**4o**	500	88	85
16		**4p**	1000	96[e]	95[f]
17		**4q**	200	83[e]	82[f]
18	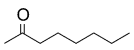	**4r**	1000	96[e]	96[f]
19		**4s**	200	95[e]	92[f]

[a] Reaction conditions: alcohol (1 mmol), **2a** (0.1–0.5 mol%), NaOAc (2.5 mol%), TFE (1 mL), N_2, reflux, 20 h. [b] Substrate/catalyst ratio. [c] Conversion was determined from the ^{1}H NMR spectrum. [d] Isolated yield. [e] Conversion was determined by GC analysis. [f] Yield was determined by GC, with decane or nonane as an internal standard.

92% isolated yield, respectively (Scheme 6). These results show that it is possible to dehydrogenate molecules that bear primary alcohol units if there is a functional group available to intercept the newly formed aldehyde.

To gain an insight into the rate-limiting step of the present Cp*Ir^{III}–NHC catalysed AD reaction the kinetic-isotope effect (KIE) was studied. Figure 8 shows the conversion-time profiles

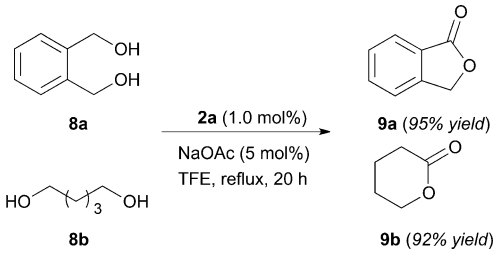

Scheme 6. AD of diols **8**.

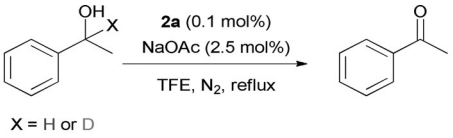

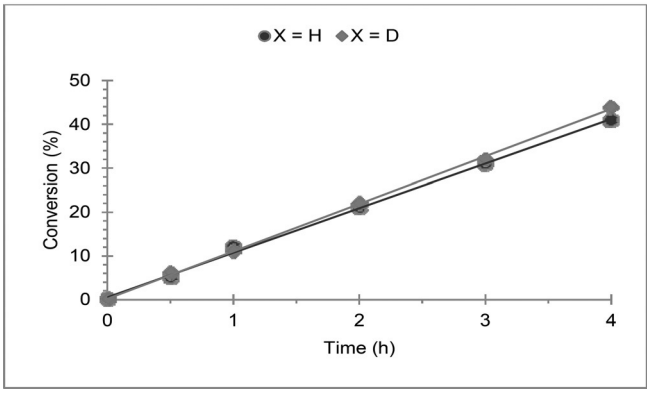

Figure 8. KIE study of the AD reaction. Deuterated (◆) or non-deuterated (●) 1-phenylethanol (1 mmol), **2a** (0.1 mol%), NaOAc (2.5 mol%), TFE (1 mL), N_2, reflux.

obtained with **3a** and its 1-deuterated analogue. Clearly, deuteration has little effect on the kinetics of the AD reaction, which suggests that C–H cleavage is not involved in the rate-limiting step. The linearity of the profiles reveals that the AD rates do not vary with time (at <50% conversion), and supports the view that the alcohol is not involved in the rate-limiting step.

To gain further insight into the reaction mechanism, the AD of **3a** with **2a** (20 mol%) in [D_3]TFE was monitored by variable temperature (VT) NMR spectroscopy (Figure 9). No product formation was observed after 30 min at room temperature. In contrast, a new peak rapidly appeared in the hydridic region of the ^{1}H NMR spectrum ($\delta = -17.4$ ppm) upon warming the reaction mixture to 50 °C along with the formation of **4a**,

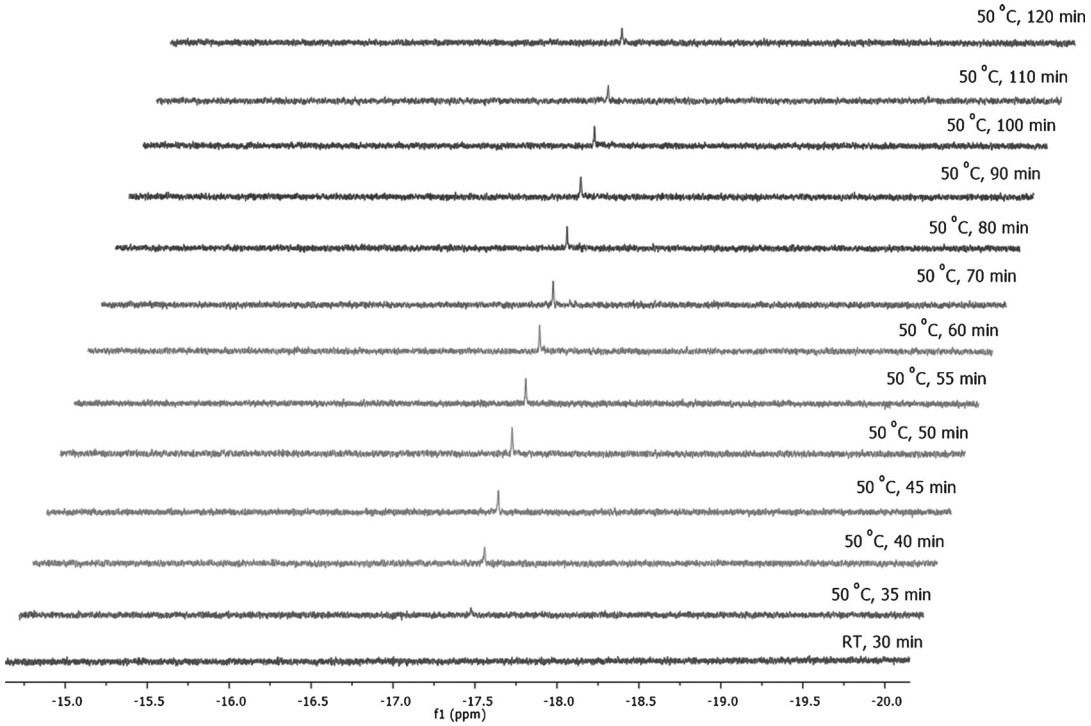

Figure 9. ^{1}H NMR hydride region of the in situ AD reaction carried out in sealed NMR tube: A solution of 1-phenylethanol (0.5 mmol), **2a** (20 mol%) and NaOAc (2.5 mol%) mixed in [D_3]TFE at RT and the ^{1}H NMR spectra was recorded after 30 min. The appearance of a new peak at $\delta = -17.4$ ppm was observed after increasing the temperature to 50 °C.

which suggested that the catalytically active species was related to this iridium hydride. The hydride remained unaltered during the VT-NMR spectroscopy experiment as conversion of **3a** to **4a** increased. These observations indicate that the rate-limiting step in the AD reaction is H_2 formation. Rate-limiting hydrogen formation has been noted for iridicycle-catalysed AD reactions, and was considered to be facilitated by TFE through protonation of the intermediate hydride.[18,25]

We also attempted to determine if there was a structure–activity relationship in the AD reaction. Thus, non-competitive dehydrogenation of a series of *para*-substituted secondary benzyl alcohols was carried out. By using the initial rate for each AD reaction, a Hammett plot of $\log(k_X/k_H)$ (k_{rel}) against the substituent constant σ_p could be constructed. Figure 10 illustrates that there is a fairly good correlation between $\log(k_X/k_H)$ and the σ_p parameters and a negative slope ($\rho = -1.03$, $R^2 = 0.99$). Because the substrate is not involved in the turnover-limiting step, this negative correlation may be indicative of a pre-equilibrium that involves the necessary substitution of the coordinated chloride anion of **2a** by the alcohol substrate, in which the substitution is favoured by more nucleophilic alcohols.

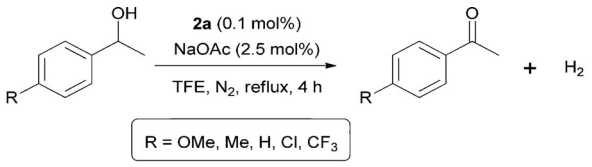

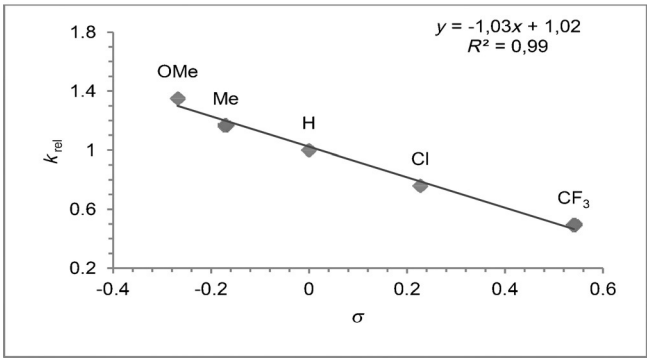

Figure 10. Hammett plots for catalyst **2a** obtained from non-competitive experiments for the AD of *para*-substituted 1-phenylethanol. Conditions: alcohol (1 mmol), **2a** (0.1 mol%), NaOAc (2.5 mol%), TFE (1 mL), N_2, reflux.

On the basis of the observations above, a possible mechanism for the AD reaction is suggested (Scheme 7). Firstly, displacement of a chloride ligand from **2a** affords an iridium–alkoxide species. This is followed by β-hydrogen elimination to give an iridium–hydride intermediate,[26] protonation of which completes the catalytic cycle. The turnover rate is determined by the protonation step, with the hydride being the catalyst resting state. All the steps appear to be reversible. An electron-rich alcohol and the introduction of a catalytic base would both be expected to shift the equilibrium of the substitution reaction to the right, which would lead to a higher concentration of the iridium–alkoxide species and, hence, a faster rate of the AD reaction.

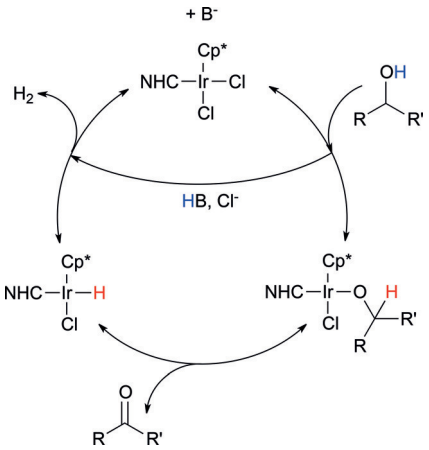

Scheme 7. Suggested mechanism for the AD of secondary alcohols catalysed by **2a**.

Conclusion

A series of Cp*Ir^{III}–NHC complexes were prepared as catalyst precursors to promote AD of secondary alcohols in TFE to give the corresponding carbonyl compounds. Variation of the NHC ligand framework allowed trends to be established. An electron-donating *para*-methoxy group on the *N*-benzyl group and imidazole as the NHC skeleton induce higher activity in this transformation. The most active catalyst **2a** was used to convert a variety of primary- and secondary alcohols to aldehydes and ketones, respectively, accompanied by the release of H_2 gas. Mechanistic observations indicated that the rate-limiting step of the AD reaction is H_2 formation. To the best of our knowledge, the TON achieved is the highest reported for the acceptorless dehydrogenative oxidation of secondary alcohols with metal–NHC catalysts. Additionally, the catalyst shows excellent selectivity for the oxidation of secondary versus primary benzylic alcohols.

Experimental Section

General

Experiments involving air- or moisture-sensitive reagents were performed under an atmosphere of purified N_2 by using standard Schlenck techniques. Unless otherwise specified, all reagents were obtained commercially and used without further purification. NMR spectra were recorded with a Bruker 400 MHz NMR spectrometer and the chemical shifts (δ) are reported in parts per million [ppm] relative to tetramethyl silane ($\delta = 0$ ppm) or $CDCl_3$ ($\delta = 77.0$ ppm) for the ^{1}H and ^{13}C NMR spectra, respectively. Melting points were measured with an X-5 Melting Point Apparatus (Beijing Tech Instrument Co.) and are uncorrected. Elemental analysis was carried out at the Microanalysis Centre, University of Liverpool. Mass spectra were obtained by Analytical Services at the Chemistry Department, University of Liverpool and the EPSRC National Mass Spectrometry Service Centre, College of Medicine, Swansea University. GC analysis was performed with an Agilent 6890N gas chromatograph equipped with a HP-5 Agilent 19091J-413 column.

Synthesis of Cp*Ir^{III}–NHC complexes

Under an argon atmosphere, a mixture of azolium salt **1** (0.5 mmol) and Ag_2O (116 mg, 0.5 mmol) was suspended in degassed, dry dichloromethane (5 mL) and stirred at ambient temperature for 1 h shielded from light. $[IrCp^*Cl_2]_2$ (198 mg, 0.25 mmol) was added to the suspension and the reaction mixture was stirred at ambient temperature for an additional 4 h. The resulting suspension was filtered over Celite®. The remaining solid was washed with dichloromethane (2×5 mL) and the filtrate was evaporated. The residue was purified by column chromatography on silica gel (9:1 dichloromethane/ethyl acetate) to afford **2** as a yellow powder.

Compound 2a: Yield: 91%, 322 mg. ^{1}H NMR (400 MHz, $CDCl_3$): $\delta =$ 7.33 (d, $J = 8.0$ Hz, 4H; Ar–*H*), 6.87 (d, $J = 8.0$ Hz, 4H; Ar–*H*), 6.62 (s, 2H; NC*H*=C*H*N), 6.03 (d, $J = 14.4$ Hz, 2H; NCH_2), 5.10 (d, $J = 14.4$ Hz, 2H; NCH_2), 3.80 (s, 6H; OCH_3), 1.65 ppm (s, 15H; $C_5(CH_3)_5$); ^{13}C NMR (100 MHz, $CDCl_3$): $\delta = 159.4$ (Ar–*C*), 156.5 (Ir–*C*), 130.1 (Ar–*C*), 128.6 (Ar–*C*), 121.5 (NCH=CHN), 114.1 (Ar-*C*), 89.0 ($C_5(CH_3)_5$), 54.1 (OCH_3), 54.1 (NCH_2), 9.3 ppm ($C_5(CH_3)_5$); HRMS (ESI+): *m/z* calcd for $C_{29}H_{35}ClIrN_2O_2$: 671.2004 $[M-Cl]^+$; found: 671.2005; elemental analysis calcd (%) for $C_{29}H_{35}Cl_2IrN_2O_2$: C 49.29, H 4.99, N 3.96; found: C 49.36, H 4.90, N 4.01.

Compound 2b: Yield: 87%, 281 mg. ^{1}H NMR (400 MHz, $CDCl_3$): $\delta =$ 7.36–7.32 (m, 10H; Ar–*H*), 6.67 (s, 2H; NC*H*=C*H*N), 6.01 (d, $J =$ 14.8 Hz, 2H; NCH_2), 5.34 (d, $J = 14.8$ Hz, 2H; NCH_2), 1.63 ppm (s, 15H; $C_5(CH_3)_5$); ^{13}C NMR (100 MHz, $CDCl_3$): $\delta = 157.5$ (Ir–*C*), 136.8 (Ar–*C*), 128.8 (Ar–*C*), 128.4 (Ar–*C*), 128.0 (Ar–*C*), 121.9 (NCH=CHN), 89.1 ($C_5(CH_3)_5$), 54.7 (NCH_2), 9.3 ppm ($C_5(CH_3)_5$); HRMS (ESI+): *m/z* calcd for $C_{27}H_{30}IrN_2$: 575.2034 $[M-H-2Cl]^+$; found: 575.2034; elemental analysis calcd (%) for $C_{27}H_{31}Cl_2IrN_2$: C 50.15, H 4.83, N 4.33; found: C 49.99, H 4.87, N 4.31.

Compound 2c: Yield: 86%, 335 mg. ^{1}H NMR (400 MHz, $CDCl_3$): $\delta =$ 7.62 (d, $J = 8.0$ Hz, 4H; Ar–*H*), 7.55 (d, $J = 8.0$ Hz, 4H; Ar–*H*), 6.68 (s, 2H; NC*H*=C*H*N), 6.30 (d, $J = 14.8$ Hz, 2H; NCH_2), 5.22 (d, $J = 14.8$ Hz, 2H; NCH_2), 1.64 ppm (s, 15H; $C_5(CH_3)_5$); ^{13}C NMR (100 MHz, $CDCl_3$): $\delta = 158.7$ (Ir–*C*), 140.5 (Ar–*C*), 130.5 (q, J(C,F) = 33.0 Hz), 128.9 (Ar–*C*), 125.7 (q, J(C,F) = 4.0 Hz), 124.7 (q, J(C,F) = 270.0 Hz), 122.2 (NCH=CHN), 89.3 ($C_5(CH_3)_5$), 54.2 (NCH_2), 9.3 ppm ($C_5(CH_3)_5$); ^{19}F NMR (376 MHz, $CDCl_3$): $\delta = -62.6$ ppm; HRMS (ESI+): *m/z* calcd for $C_{29}H_{29}ClF_6IrN_2$: 747.1545 $[M-Cl]^+$; found: 747.1535; elemental analysis calcd (%) for $C_{29}H_{29}Cl_2F_6IrN_2$: C 44.50, H 3.73, N 3.58; found: C 44.43, H 3.75, N 3.55.

Compound 2d: Yield: 90%, 318 mg. ^{1}H NMR (400 MHz, $CDCl_3$): $\delta =$ 7.41 (d, $J = 8.0$ Hz, 4H; Ar–*H*), 6.85 (d, $J = 8.0$ Hz, 4H; Ar–*H*), 5.61 (d, $J = 14.0$ Hz, 2H; NCH_2), 4.38 (d, $J = 14.0$ Hz, 2H; NCH_2), 3.79 (s, 6H; OCH_3), 3.43 (t, $J = 9.6$ Hz, 2H; NCH_2CH$_2$N), 3.28 (t, $J = 9.6$ Hz, 2H; NCH$_2$CH_2N), 1.66 ppm (s, 15H; $C_5(CH_3)_5$); ^{13}C NMR (100 MHz, $CDCl_3$): $\delta = 186.5$ (Ir–*C*), 159.1 (Ar–*C*), 129.8 (Ar–*C*), 128.6 (Ar–*C*), 113.8 (Ar–*C*), 89.4 ($C_5(CH_3)_5$), 55.3 (OCH_3), 55.1 (NCH_2), 48.6 (NCH_2CH$_2$N), 9.3 ppm ($C_5(CH_3)_5$); HRMS (ESI+): *m/z* calcd for $C_{29}H_{37}ClIrN_2O_2$: 673.2166 $[M-Cl]^+$; found: 673.2158; elemental analysis calcd (%) for $C_{29}H_{37}Cl_2IrN_2O_2$: C 49.15, H 5.26, N 3.95; found: C 49.13, H 5.31, N 3.99.

Compound 2e: Yield: 81%, 305 mg. ^{1}H NMR (400 MHz, $CDCl_3$): $\delta =$ 7.07 (d, $J = 8.8$ Hz, 4H; Ar–*H*), 6.99 (t, $J = 6.0$ Hz, 2H; Ar–*H*), 6.92 (dd, $J = 6.0$, 3.2 Hz, 2H; Ar–*H*), 6.85 (d, $J = 8.8$ Hz, 4H; Ar–*H*), 6.18 (d, $J = 16.4$ Hz, 2H; NCH_2), 5.90 (d, $J = 16.4$ Hz, 2H; NCH_2), 3.79 (s, 6H; OCH_3), 1.55 ppm (s, 15H; $C_5(CH_3)_5$); ^{13}C NMR (100 MHz, $CDCl_3$): $\delta = 172.0$ (Ir–*C*), 158.8 (Ar–*C*), 135.3 (Ar–*C*), 128.8 (Ar–*C*), 127.6 (Ar–*C*), 122.9 (Ar–*C*), 114.1 (Ar–*C*), 112.5 (Ar–*C*), 90.0 ($C_5(CH_3)_5$), 55.3 (OCH_3), 53.0 (NCH_2), 9.2 ppm ($C_5(CH_3)_5$); HRMS (ESI+): *m/z* calcd for $C_{33}H_{35}ClIrN_2O_2$: 719.2009 $[M-2H-Cl]^+$; found: 719.2005; elemental

analysis calcd (%) for $C_{33}H_{37}Cl_2IrN_2O_2$: C 52.37, H 4.93, N 3.70; found: C 52.29, H 4.88, N 3.72.

Compound 2f: Yield: 75%, 283 mg. ^{1}H NMR (400 MHz, $CDCl_3$): $\delta =$ 6.95 (d, $J = 8.4$ Hz, 4H; Ar–*H*), 6.91 (d, $J = 8.4$ Hz, 4H; Ar–*H*), 6.32 (d, $J = 16.8$ Hz, 2H; NCH_2), 5.43 (d, $J = 16.8$ Hz, 2H; NCH_2), 3.83 (s, 6H; OCH_3), 1.43 ppm (s, 15H; $C_5(CH_3)_5$); ^{13}C NMR (100 MHz, $CDCl_3$): $\delta =$ 161.9 (Ir–*C*), 158.9 (Ar–*C*), 128.8 (Ar–*C*), 126.5 (Ar–*C*), 118.9 (Ar–*C*), 114.2 (Ar–*C*), 89.8 ($C_5(CH_3)_5$), 55.3 (OCH_3), 53.7 (NCH_2), 9.1 ppm ($C_5(CH_3)_5$); HRMS (ESI+): *m/z* calcd for $C_{29}H_{35}Cl_2IrN_3O_2$: 720.1725 $[M-2H-2Cl+NH_4]^+$; found: 720.1716; elemental analysis calcd (%) for $C_{29}H_{33}Cl_4IrN_2O_2$: C 44.91, H 4.29, N 3.61; found: C 44.98, H 4.32, N 3.57.

Synthesis of 2a′

Complex **2a** (141 mg, 0.2 mmol) and NaOAc (82 mg, 1.0 mmol) were suspended in dichloromethane (5 mL) and the mixture was stirred at ambient temperature for 12 h. The solvent was evaporated then the residue was purified by column chromatography to give **2a′** (90%, 120 mg) as a yellow powder. ^{1}H NMR (400 MHz, $CDCl_3$): $\delta = 7.36$ (d, $J = 8.4$ Hz, 2H; Ar–*H*), 7.27 (d, $J = 2.8$ Hz, 1H; Ar–*H*), 6.87–6.82 (m, 4H; Ar–*H* and NC*H*=C*H*N), 6.59 (d, $J = 1.6$ Hz, 1H; Ar–*H*), 6.40 (dd, $J = 8.0$, 2.4 Hz, 1H; Ar–*H*), 5.95 (d, $J = 14.0$ Hz, 1H; NCH_2), 4.99 (d, $J = 14.0$ Hz, 1H; NCH_2), 4.83 (d, $J = 14.0$ Hz, 1H; NCH_2), 4.62 (d, $J = 14.0$ Hz, 1H; NCH_2), 3.80 (s, 3H; OCH_3), 3.78 (s, 3H; OCH_3), 1.69 ppm (s, 15H; $C_5(CH_3)_5$); ^{13}C NMR (100 MHz, $CDCl_3$): $\delta = 159.4$ (Ar–*C*), 158.3 (Ar–*C*), 156.7 (Ir–$C_{carbene}$), 146.1 (Ir–C_{Ar}), 131.7 (Ar–*C*), 130.6 (Ar–*C*), 128.6 (Ar–*C*), 125.9 (Ar–*C*), 124.6 (Ar–*C*), 120.2 (NC*H*=C*H*N), 120.2 (NC*H*=C*H*N), 114.0 (Ar–*C*), 108.0 (Ar–*C*), 90.3 ($C_5(CH_3)_5$), 56.7 (OCH_3), 55.3 (NCH_2), 55.2 (OCH_3), 52.8 (NCH_2), 9.6 ppm ($C_5(CH_3)_5$); elemental analysis calcd (%) for $C_{29}H_{34}ClIrN_2O_2$: C 51.97, H 5.11, N 4.18; found: C 52.04, H 5.07, N 4.21; HRMS (ESI+): *m/z* calcd for $C_{29}H_{33}ClIrN_2O_2$: 669.1847 $[M-H]^+$; found: 669.1827.

General procedure for the acceptorless dehydrogenative oxidation of 3a

Alcohol **3a** (1.0 mmol), additive (1.0–10 mol%) and **2a** (0.05–1.0 mol%) were dissolved in TFE (1 mL) in a carousel reaction tube. The contents of the tube were degassed then reaction mixture was heated at reflux under N_2 for 2–20 h. The reaction mixture was cooled to RT and the solvent was evaporated under reduced pressure. The conversion of **3a** was determined by ^{1}H NMR spectroscopy.

X-ray crystallography

Crystallographic data and refinement are provided in Tables S1–S7 in the Supporting Information. CCDC 1424271 (<**2a**), 1470605 (**2b**),1470606 (**2c**),1470607 (**2d**),1470608 (**2e**),1470609 (**2f**) and 1470610 (**2a′**) contain the supplementary crystallographic data for this paper. These data can be obtained free of charge from The Cambridge Crystallographic Data Centre via www.ccdc.cam.ac.uk/data_request/cif.

Acknowledgements

The authors thank the Scientific and Technological Research Council of Turkey (TUBITAK) BIDEB-2219 for postdoctoral fellowships (D.G. and S.G.). Mass spectrometry data were acquired at the EPSRC UK National Mass Spectrometry Facility at Swansea University. We also thank Dr. R. Sebastian Sprick for performing the H_2-evolution experiments and Dr. Konstantin Luzyanin for performing the VT-NMR experiments.

Keywords: acceptorless dehydrogenation · alcohols · carbenes · iridium · oxidation

[1] a) O. Kühl, *Functionalised N-Heterocyclic Carbene Complexes*, Wiley-VCH, Weinheim, **2010**; b) S. Díez-González, *N-Heterocyclic Carbenes: From Laboratory Curiosities to Efficient Synthetic Tools*, Royal Society of Chemistry, Cambridge, **2011**; c) S. P. Nolan, *N-Heterocyclic Carbenes: Effective Tools for Organometallic Synthesis*, Wiley-VCH, Weinheim, **2014**; d) M. N. Hopkinson, C. Richter, M. Schedler, F. Glorius, *Nature* **2014**, *510*, 485.

[2] a) A. Pontes da Costa, M. Viciaono, M. Sanau, S. Merino, J. Tejeda, E. Peris, B. Royo, *Organometallics* **2008**, *27*, 1305; b) X. Gong, H. Zhang, X. Li, *Tetrahedron Lett.* **2011**, *52*, 5596; c) A. Sølvhøj, R. Madsen, *Organometallics* **2011**, *30*, 6044.

[3] X. Xie, H. V. Hyunh, *ACS Catal.* **2015**, *5*, 4143.

[4] N. Ortega, C. Richter, F. Glorius, *Org. Lett.* **2013**, *15*, 1776.

[5] a) A. Maggi, R. Madsen, *Organometallics* **2012**, *31*, 451; b) B. Saha, S. M. W. Rahaman, P. Dow, G. Sengupta, J. K. Bera, *Chem. Eur. J.* **2014**, *20*, 6542.

[6] a) S. Shahane, C. Fischmeister, C. Bruneau, *Catal. Sci. Technol.* **2012**, *2*, 1425; b) D. Canseco-Gonzalez, M. Albrecht, *Dalton Trans.* **2013**, *42*, 7424; c) V. Leigh, D. J. Carleton, J. Olguin, H. Mueller-Bunz, L. J. Wright, M. Albrecht, *Inorg. Chem.* **2014**, *53*, 8054; d) A. R. Naziruddin, C.-S. Zhuang, W.-L. Lin, W.-S. Hwang, *Dalton Trans.* **2014**, *43*, 5335; e) S. Sabater, J. A. Mata, E. Peris, *ACS Catal.* **2014**, *4*, 2038.

[7] a) I. E. Marko, P. R. Giles, M. Tsukazaki, S. M. Brown, C. J. Urch, *Science* **1996**, *274*, 2044; b) R. A. Sheldon, I. W. C. E. Arends, G.-J. ten Brink, A. Dijksman, *Acc. Chem. Res.* **2002**, *35*, 774; c) G. Csjernyik, A. H. Ell, L. Fadini, B. Pugin, J.-E. Bäckvall, *J. Org. Chem.* **2002**, *67*, 1657; d) B. Jiang, Y. Feng, E. A. Ison, *J. Am. Chem. Soc.* **2008**, *130*, 14462; e) B. Karimi, F. K. Esfahani, *Chem. Commun.* **2009**, 5555.

[8] a) K. Sato, M. Aoki, J. Takagi, R. Noyori, *J. Am. Chem. Soc.* **1997**, *119*, 12386; b) R. Noyori, M. Aoki, K. Sato, *Chem. Commun.* **2003**, 1977; c) B. Join, K. Möller, C. Ziebart, K. Schröder, D. Gördes, K. Thurow, A. Spannenberg, K. Junge, M. Beller, *Adv. Synth. Catal.* **2011**, *353*, 3023; d) W. Dai, Y. Lv, L. Wang, S. Shang, B. Chen, G. Li, S. Gao, *Chem. Commun.* **2015**, *51*, 11268; e) D. Shen, C. Miao, D. Xu, C. Xia, W. Sun, *Org. Lett.* **2015**, *17*, 54.

[9] a) M. L. S. Almeida, M. Beller, G.-Z. Wang, J.-E. Bäckvall, *Chem. Eur. J.* **1996**, *2*, 1533; b) K. Fujita, S. Furukawa, R. Yamaguchi, *J. Organomet. Chem.* **2002**, *649*, 289; c) F. Hanasaka, K. Fujita, R. Yamaguchi, *Organometallics* **2004**, *23*, 1490; d) F. Hanasaka, K. Fujita, R. Yamaguchi, *Organometallics* **2005**, *24*, 3422; e) F. Hanasaka, K. Fujita, R. Yamaguchi, *Organometallics* **2006**, *25*, 4643; f) M. G. Coleman, A. N. Brown, B. A. Bolton, H. Guan, *Adv. Synth. Catal.* **2010**, *352*, 967; g) S. Sabater, J. A. Mata, E. Peris, *Organometallics* **2012**, *31*, 6450.

[10] a) Y. Choi, A. H. R. MacArthur, M. Brookhart, A. S. Goldman, *Chem. Rev.* **2011**, *111*, 1761; b) T. Suzuki, *Chem. Rev.* **2011**, *111*, 1825; c) C. Gunanathan, D. Milstein, *Science* **2013**, *341*, 249; d) M. Trincado, D. Banerjee, H. Grützmacher, *Energy Environ. Sci.* **2014**, *7*, 2464; e) S. Werkmeister, J. Neumann, K. Junke, M. Beller, *Chem. Eur. J.* **2015**, *21*, 12226; f) S. Kaufhold, L. Petermann, R. Staehle, S. Rau, *Coord. Chem. Rev.* **2015**, *304–305*, 73; g) Q. Yang, Q. Wang, Z. Yu, *Chem. Soc. Rev.* **2015**, *44*, 2305.

[11] Iron-catalysed AD: a) M. Kamitani, M. Ito, M. Itazaki, H. Nakazawa, *Chem. Commun.* **2014**, *50*, 7941; b) H. Song, B. Kang, S. H. Hong, *ACS Catal.* **2014**, *4*, 2889; c) S. Chakraborty, P. O. Lagaditis, M. Förster, E. A. Bielinski, N. Hazari, M. C. Holthausen, W. D. Jones, S. Schneider, *ACS Catal.* **2014**, *4*, 3994; d) P. J. Bonitatibus Jr, S. Chakraborty, M. D. Doherty, O. Siclovan, W. D. Jones, G. L. Soloveichik, *Proc. Natl. Acad. Sci. USA* **2015**, *112*, 1687.

[12] Ruthenium-catalysed AD: a) J. Zhang, M. Gondelman, L. J. W. Shimon, H. Rozenberg, D. Milstein, *Organometallics* **2004**, *23*, 4026; b) J. Zhang, E. Balaraman, G. Leitus, D. Milstein, *Organometallics* **2011**, *30*, 5716; c) S. Muthaiah, S. H. Hong, *Adv. Synth. Catal.* **2012**, *354*, 3045; d) G. Zeng, S. Sakaki, K. Fujita, H. Sano, R. Yamaguchi, *ACS Catal.* **2014**, *4*, 1010.

[13] Osmium-catalysed AD: a) M. Baratta, G. Bossi, E. Putignano, P. Rigo, *Chem. Eur. J.* **2011**, *17*, 3474; b) M. Bertoli, A. Choualeb, A. J. Lough, B. Moore, D. Spasyuyk, D. G. Gusev, *Organometallics* **2011**, *30*, 3479.

[14] Rhodium catalysed AD: a) D. Morton, D. J. Cole-Hamilton, *J. Chem. Soc. Chem. Commun.* **1987**, 248; b) T. Zweifel, J.-V. Naubron, H. Grützmacher, *Angew. Chem. Int. Ed.* **2009**, *48*, 559; *Angew. Chem.* **2009**, *121*, 567.

[15] Iridium-catalysed AD: a) K. Fujita, N. Tanino, R. Yamaguchi, *Org. Lett.* **2007**, *9*, 109; b) A. M. Royer, T. B. Rauchfuss, D. L. Grey, *Organometallics* **2010**, *29*, 6763; c) S. Musa, I. Shaposhnikov, S. Cohen, D. Gelman, *Angew. Chem. Int. Ed.* **2011**, *50*, 3533; *Angew. Chem.* **2011**, *123*, 3595; d) K. Fujita, T. Yoshida, Y. Imori, R. Yamaguchi, *Org. Lett.* **2011**, *13*, 2278; e) M. Nielsen, A. Kammer, D. Cazzula, H. Junge, S. Gladiali, M. Beller, *Angew. Chem. Int. Ed.* **2011**, *50*, 9593; *Angew. Chem.* **2011**, *123*, 9767; f) R. Kawahara, K. Fujita, R. Yamaguchi, *J. Am. Chem. Soc.* **2012**, *134*, 3643; g) R. Kawahara, K. Fujita, R. Yamaguchi, *Angew. Chem. Int. Ed.* **2012**, *51*, 12790; *Angew. Chem.* **2012**, *124*, 12962; h) A. V. Polukeev, P. V. Petrovskii, A. S. Peregudov, M. G. Ezernitskaya, A. A. Koridze, *Organometallics* **2013**, *32*, 1000; i) A. H. Ngo, M. J. Adams, L. H. Do, *Organometallics* **2014**, *33*, 6742.

[16] H. M. J. Wang, I. J. B. Lin, *Organometallics* **1998**, *17*, 972.

[17] a) A. Azua, J. A. Mata, E. Peris, F. Lamaty, J. Martinez, E. Colacino, *Organometallics* **2012**, *31*, 3911; b) X.-H. Zhu, L.-H. Cai, C.-X. Wang, Y.-N. Wang, X. Q. Guo, X.-F. Hou, *J. Mol. Catal. A* **2014**, *393*, 134; c) D. Gülcemal, S. Gülcemal, C. M. Robertson, J. Xiao, *Organometallics* **2015**, *34*, 4394.

[18] J. Wu, D. Talwar, S. Johnston, M. Yan, J. Xiao, *Angew. Chem. Int. Ed.* **2013**, *52*, 6983; *Angew. Chem.* **2013**, *125*, 7121.

[19] R. E. Mesmer, K. M. Palen, C. F. Baes Jr, *Inorg. Chem.* **1973**, *12*, 89.

[20] Formation of H_2 was confirmed by GC analysis (see the Supporting Information).

[21] Z. M. Heiden, T. B. Rauchfuss, *J. Am. Chem. Soc.* **2007**, *129*, 14303.

[22] a) R. Corberán, M. Sanaú, E. Peris, *J. Am. Chem. Soc.* **2006**, *128*, 3974; b) R. Corberán, M. Sanaú, E. Peris, *Organometallics* **2006**, *25*, 4002.

[23] M. H. S. A. Hamid, P. A. Slatford, J. M. J. Williams, *Adv. Synth. Catal.* **2007**, *349*, 1555.

[24] a) T. Suzuki, K. Morita, M. Tsuchida, K. Hiroi, *Org. Lett.* **2002**, *4*, 2361; b) J. Zhao, J. F. Hartwig, *Organometallics* **2005**, *24*, 2441; c) K.-N. T. Tseng, J. W. Kampf, N. K. Szymczak, *Organometallics* **2013**, *32*, 2046; d) K. Fujita, W. Ito, R. Yamaguchi, *ChemCatChem* **2014**, *6*, 109.

[25] Q. Zou, C. Wang, J. Smith, D. Xue, J. Xiao, *Chem. Eur. J.* **2015**, *21*, 9656.

[26] H.-Y. T. Chen, C. Wang, X. Wu, X. Jiang, C. R. A. Catlow, J. Xiao, *Chem. Eur. J.* **2015**, *21*, 16564.

Received: April 8, 2016
Published online on June 20, 2016